

1 ENVIRONMENTAL AND ANTHROPOGENIC FACTORS CO-SHAPE COMMUNITY- 2 LEVEL PLANT SPECIES RICHNESS ACROSS THE WESTERN SIBERIAN ARCTIC

3 Factors co-shape W. Siberian tundra PSR

4 **Abstract**

5 **Aim**

6 The Arctic ecosystem and its species are exposed to amplified climate warming and in some
7 regions to rapidly developing economic activity. This study strives to identify, model and map
8 the patterns of community-level plant species richness in the Western Siberian Arctic and to
9 estimate the relative impact of environmental and anthropogenic factors driving these patterns.
10 With our results and methods, we aim at contributing towards conservation efforts for arctic
11 species richness.

12 **Location**

13 Western Siberian Arctic, Russia.

14 **Methods**

15 We investigated the relative impact of environmental, topographic and anthropogenic factors on
16 community-level plant species richness of the Western Siberian Arctic, using macroecological
17 models trained with an extensive, newly assembled geobotanical dataset. We included vascular
18 plants, mosses and lichens in our analysis, as non-vascular plants substantially contribute to
19 species richness and ecosystem functions in the Arctic.

20 **Results**

21 We found that the mean community-level plant species richness in this vast Arctic region does
22 not decrease with increasing latitude. Instead, we identified an increase in species richness
23 from South-West to North-East, which can be explained by climatic, topographical and
24 anthropogenic factors. We found that lowest species richness is associated with a medium (30
25 to 50 km) distance to infrastructure while neighboring (0 to 10 km) and remote (\approx 100 km) areas

26 have relatively high species richness. We also show that the existing protected areas cover only
27 a small part of the areas with the highest species richness.

28 **Conclusions**

29 Our results reveal complex spatial patterns of community-level species richness in the Western
30 Siberian Arctic. We suggest that the impact of economic activities on species richness is
31 ambiguous and not limited to areas directly affected by infrastructure. We show that while
32 community-level plant species richness is mostly driven by non-anthropogenic factors, human
33 activities also contribute to the heterogeneous distribution of community-level species richness
34 on a broad scale. Our approach and results can be used to develop nature protection strategies
35 for other arctic regions facing similar challenges.

36

37 **Keywords:** Arctic, macroecological modeling, Arctic Vegetation Archive, community-level plant
38 species richness, anthropogenic impact on biodiversity, tundra vegetation, anthropogenic
39 change.

40 **Introduction**

41 The documentation of Arctic plant diversity and its distribution under global change is one of the
42 key priorities of international science and policy agendas as coordinated by the Conservation of
43 Arctic Flora and Fauna (CAFF, 1997) of the Arctic Council and the International Arctic Science
44 Committee (IASC). This information is urgently needed for the identification of Arctic biodiversity
45 hotspots, which are a major target for nature protection and conservation (UN Convention on
46 Biological diversity, CBD) (CBD, 1992). Plant diversity in the Arctic is usually studied at regional
47 (hundreds of square kilometres), local (square kilometres) and community (square meters)
48 levels. Despite Arctic regional and (to a lesser extent) local plant diversity being relatively well
49 documented, the community-level distribution of plant diversity across broad spatial extents and
50 its drivers remains understudied, especially in the Siberian part of the Arctic (Walker et al. 1994;

51 Daniëls et al. 2005; Daniëls et al., 2013; Khitun et al. 2016). Yet, disentangling the relative
52 impact of the environmental and anthropogenic drivers of diversity at the community level is
53 important for understanding the distribution of Arctic vegetation and predicting its response to
54 global change.

55

56 Species richness across plant communities in the Arctic is determined by an interaction of local
57 abiotic factors such as soil moisture, meso- and microrelief, wind speed and exposure,
58 permafrost and soil conditions (Schultz, 2005; Iturrate-Garcia et al., 2016; Walker et al., 2019),
59 which can promote high heterogeneity among communities at small spatial scales. This
60 heterogeneity is often larger than intra-regional differences between communities belonging to
61 the same vegetation type (Khitun, 1998; Khitun and Rebristaya, 1998). Furthermore,
62 anthropogenic factors play an increasingly important role in shaping Arctic vegetation, changing
63 community composition, threatening some local species (especially, lichens and mosses) and
64 simultaneously increasing total plant species richness through introduction of new species and
65 habitat change (Forbes 1995; 1997; Rebristya and Khitun, 1998; Nellemann et al., 2001; Red
66 book of YANAO, 2010; Daniëls et al. 2013, Povoroznyuk et al. 2022).

67

68 The Western Siberian tundra is a rapidly transforming region of the Arctic (Kumpula et al. 2011,
69 2012; Walker et. al, 2012; Kozlova, 2013). The combination of multiple interacting factors
70 including climate change, infrastructure expansion, fossil fuel extraction (Skipin, 2014), reindeer
71 pressure (Kryazhimskii et al., 2011; Egelkraut et al., 2020; Veselkin et al., 2021) and species
72 invasions, contributes to large-scale ecosystem degradation within and beyond areas directly
73 affected by economic activity (Forbes et al., 2009; Golovatin et al., 2012). The high landscape
74 homogeneity (Rebristaya, 2013) at broad spatial scales (about 300'000 km²) contrasting with
75 the uneven spatial distribution of anthropogenic impacts make the Western Siberian tundra a

76 natural laboratory for studying the relative impact of environmental and anthropogenic drivers on
77 tundra flora and vegetation across biological, temporal, and spatial scales.

78
79 Most of the botanical research in the Western Siberian tundra was conducted at the site level,
80 following the 'local flora' methodology (Rebristaya et al., 1989; Rebristaya and Khitun, 1994,
81 1998; Khitun and Rebristaya, 1998; Khitun, 2002, 2003; Rebristaya, 2013; Khitun et al., 2016).
82 This methodology is based on a complete assessment of vascular plant species in an area of
83 100-300 km². There are 42 local floras described across the Western Siberian tundra, but their
84 distribution is uneven: about two thirds of the local floras were described on the Yamal
85 peninsula, while other areas are poorly sampled. Local species pools vary widely: from 215
86 species in Layakha, west of Taz peninsula (Fig. 1), subzone E (Rebristaya et al., 1989; CAVM,
87 2003), and 209 species in Chugoryakha, south-west of Gydan (Fig.1), subzone E (Rebristaya
88 and Khitun 1994; CAVM, 2003), to 75 species on Bely island, subzone B (Rebristaya, 1995;
89 CAVM, 2003). Generally, regional species richness declines with latitude, but areas at the same
90 latitude at Gydan have richer floras than at Yamal by 20 to 30 species (Khitun, 1998; Khitun,
91 2016; Rebristaya 2013). Although overall summer warmth has been identified as the main
92 contributing factor to floristic richness gradients, other factors such as soil acidity, glaciation and
93 sea level history of the area and its flora are also considered important (Walker et al. 2005;
94 Khitun, 1998, 2016).

95
96 While earlier studies based on local floristic data provide important insight into regional vascular
97 plant species richness, we still lack an understanding of which factors are structuring the
98 species richness at the fine-grained community level across the Western Siberian Arctic and
99 how climate, topographic and anthropogenic factors combine to impact community species
100 richness across broad spatial extents. Large-scale quantitative studies of community-level
101 species richness have not been carried out in Western Siberia, where existing studies rely either

102 on traditional geobotanical methods or are limited to smaller areas (Khitun, 1998; Forbes and
103 Sumina, 1999; Rebristaya 2013). Here, based on a newly assembled, large geobotanical data
104 set, we aim to identify the main drivers and map the patterns of community-level plant species
105 richness, including vascular plants, mosses and lichens, in the Western Siberian tundra and the
106 environmental and anthropogenic forces driving these patterns. We estimate the relative impact
107 of different modern and historical environmental factors on plot-level community species
108 richness using macroecological models. We model the distribution of mean plant species
109 richness across the area and compare these predictions to previous geobotanical studies. We
110 also discuss how economic activities contribute to the community-level patterns of plant species
111 richness. In our study, we posit four core hypotheses: 1) climate factors (including paleoclimate)
112 are more important in explaining patterns of community-level species richness than topographic
113 factors, 2) anthropogenic factors are as important predictors as natural factors, 3) community-
114 level plant species richness in the area follows the latitudinal diversity gradient , and 4) current
115 protected areas do not sufficiently well cover regions with high species richness.

116 **Methods**

117 The objective of our research is estimating the distribution of plant species richness at the
118 community level across the Western Siberian tundra. To this end, we used macroecological
119 models, predicting mean plot-level plant species richness as a function of environmental factors
120 (Guisan and Rahbek, 2011; Guisan et al., 2017). We also estimated the role of anthropogenic
121 factors, using distance from infrastructure as a proxy for anthropogenic impact.

122

123 **Study area**

124 The Western Siberian tundra is located in the northern part of the Western Siberian plain and
125 covers slightly more than 300'000 km². The area has a low plant species richness at the

126 regional level because of its landscape properties and geoclimatic history. According to the
127 floristic classification by Yurtsev (1994), used in the Circumpolar Arctic Vegetation map (CAVM
128 team, 2003), the area belongs to the European-West-Siberian province (Yamal-Gydan
129 subprovince) of the Arctic floristic region (Yurtsev, 1994). In comparison with neighboring
130 subprovinces, Yamal-Gydan is characterized by almost complete absence of endemism,
131 extremely low vascular plant species richness (the lowest in continental Russia), and a lack of
132 many montane species (Yurtsev, 1994; Khitun, 1998; Sekretareva, 1999; Rebristaya, 2013;
133 Daniëls et al., 2013). In total, the province harbors about 450 species of vascular plants
134 (Koroleva et al., 2011), 276 species of mosses (Chernyadyeva, 2001; Voronova and
135 Dyachenko, 2018) and 250 species of lichens (Magomedova et al., 2006). The flora of the area
136 was shaped by Quaternary climate oscillations as well as glaciations and marine
137 transgressions, which had an especially strong impact on Yamal (Rebristaya 2013; Stewart et
138 al., 2016). Landscape homogeneity, high soil acidity, and absence of bedrock exposure also
139 contribute to observed low species richness (Khitun 1998; Rebristaya, 2013).

140

141 Geobotanical plots

142 To estimate community-level species richness we used geobotanical data from the Russian
143 Arctic Vegetation Archive (Ermokhina et al., 2022). These data consist of 1483 Braun Blanquet
144 plots established in homogenous vegetation collected during 2005-2017 field campaigns in the
145 Western Siberian tundra (Fig. 1) (Zemlianskii et al., 2023). The data were collected following the
146 standard international Arctic Vegetation Archive protocol (Walker et al., 2013, 2016, 2018) and
147 include full species lists of vascular plants and (contrary to most other existing floristic studies of
148 the area) also bryophytes and lichens (Elven, 2011; Reynolds et al., 2013). For the 12 major
149 sites (100-150 km² sub-areas in which more than 60 plots were sampled), we collected data
150 representative for all vegetation types present in the area (at least 5 plots of related

151 communities per site). In addition, we used 10 minor sites with 4-21 plots per site. The plot size
152 varied from 25 to 100 m² depending on community characteristics (Matveeva, 1998). We
153 divided plots into two classes, large plots (100m²) and small plots (less than 100m²), to test for
154 the effect of plot size on species richness.

155
156 The plot-level species richness, which we calculated by plot-wise summing species richness of
157 vascular plants, mosses and lichens (liverworts data was omitted because of uneven
158 identification quality across the database) was used to build regression-type macroecological
159 models. The response variable of our models was total species richness per community. To
160 estimate latitudinal trends at the site-level, we also inferred lichen, moss, vascular plants and
161 total species richness for each major site.

162

163 Environmental variables

164 For each geobotanical plot, we extracted corresponding data from a set of 48 environmental
165 predictors describing climate, topography, vegetation, and anthropogenic impact (Appendix
166 Table S1). Climatic predictors included wind speed from the Global Wind Atlas
167 (<https://globalwindatlas.info/>), 19 bioclimatic variables (seasonal and annual statistics of
168 temperature and precipitation) from CHELSA (Karger et al., 2017), mean ground temperature
169 from ESA Global permafrost project (Obu, et al., 2019), and annual statistics of climate moisture
170 index, total cloud cover, potential evapotranspiration, site water balance, and growing degree
171 days from CHELSA-BIOCLIM+ (Brun et al., 2022). Topographic predictors included altitude
172 (incl. standard deviation of altitude), topographic position index, log-transformed slope, and
173 aspect, which were derived from the Arctic digital elevation model (Morin et al., 2016; Porter et
174 al., 2018) and topographic wetness index (Marthews et al., 2015). Mean normalized difference
175 vegetation index (NDVI) for the period July-August 2019-2020 as observed by MODIS was used

176 as vegetation-related predictor (<https://modis.gsfc.nasa.gov/>). A detailed list of predictors can be
177 seen in Appendix Table S1. All predictors were reprojected, resampled, and aligned to a
178 consistent grid in ESRI:102025 projection with 1000 m horizontal resolution. From this set of
179 predictors, we selected 14 predictors for analysis based on univariate predictive performance
180 (see Appendix Table S1), limited collinearity (absolute pairwise Pearson correlation coefficients
181 <0.7), and ecological relevance (different types of factors such as temperature, wind, relief and
182 precipitation were represented with at least one predictor, and factors with direct effects were
183 preferred over factors with indirect effects). We also classified the plots to small (less than
184 100m²) and large (100m²) to correct for the potential effect of plot size on species richness.
185 Finally, we used distance to infrastructure as a proxy for anthropogenic impact, combining
186 industrial activities and the resulting species invasion and increase of reindeer pressure into one
187 single predictor. To this end, we downloaded all the available data for roads, railroads,
188 settlements, industrial sites, and airports from OpenStreetMap (<https://www.openstreetmap.org>)
189 and converted them to points. Then, we calculated the distance between each raster cell and
190 the closest infrastructure point. Raster layers were reprojected in QGIS (version 3.12,
191 <https://www.qgis.org/>) while the resampling and predictor selection was conducted in R (version
192 4.1.2, R Core Team, 2021) using the package raster (Bivand et al., 2021).

193

194 In addition to modern climate, we investigated the effect of five paleoclimatic variables (mean
195 annual temperature, annual precipitation sum, paleo-elevation, distance to land ice, and
196 maximum (latest) year in time-series where the location was covered by land ice) from the Last
197 Glacial Maximum period using the CHELSA-TraCE21k dataset (Karger et al., 2021). The data
198 for our geobotanical plots was obtained through an R script
199 (https://github.com/jakobjassmann/cryo_db_v2). We assessed the univariate predictive
200 performance of the historical predictors and assured limited collinearity to modern climate
201 predictors.

202

203 Fitting macroecological models

204 We modeled species richness as a function of non-anthropogenic predictors using four different
205 model algorithms: random forest (RF), gradient boosting machines (GBMs), generalized linear
206 models (GLMs), and generalized additive models (GAMs) (see Appendix Table S1). For RF, we
207 fitted 500 regression trees, considering three predictors for each tree. For GBMs, we set the
208 number of trees to 80, the minimum number of data points per leaf to 10, the learning rate to 0.1
209 and the error distribution was to 'poisson'. For GLMs and GAMs we assumed a Poisson error
210 distribution and used the 'log' link function. For GLMs, we defined a linear and a quadratic term
211 for each predictor. For GAMs, we used smooth terms with four degrees of freedom. For GLMs
212 and GAMs, we step-wise optimized the Akaike information criterion by removing uninformative
213 predictor terms from the model equation. Macroecological models were fitted in the R
214 environment (version 4.1.2) using the packages randomForest (Liaw and Wiener, 2002), gbm
215 (Greenwell et al., 2020), and gam (Hastie, 2020).

216

217 Model validation and performance

218 We used 5-fold cross-validation to estimate model performance. Agreement between observed
219 and predicted species richness was assessed using Spearman correlation coefficients and
220 mean absolute error (MAE).

221

222 Spatial projections

223 We produced plant species richness maps based on ensembles of spatial projections. For all
224 fitted models that fulfilled the performance criterion (Table 1), we generated ensemble spatial
225 projections of species richness across the study area. Ensembles were generated using the
226 mean of modelled species richness among the different algorithms. In addition, we derived the

227 model disagreement between algorithms as the prediction span (i.e., maximum - minimum
228 predicted species richness among algorithms per pixel). Finally, we intersected the obtained
229 richness map with a shapefile of existing protected areas borders (CAFF, 2010).

230

231 Estimation of anthropogenic impact related to economic activities

232 To assess the role of human impact related to economic activity, we tested the predictive power
233 of distance to infrastructure derived from Open Street Maps (<https://www.openstreetmap.org/>)
234 for species richness and examined its response curve (Appendix Fig. 1). To this end, we added
235 distance to infrastructure as a predictor to macroecological models and updated the predictions
236 of species richness. To disentangle anthropogenic impact from environmental factors we
237 produced maps with anthropogenic impact set to zero (we indicated the maximum distance to
238 infrastructure which was found to be 115.285 km) and compared the obtained maps with
239 predictions made using environmental data only. To estimate potential influence of economic
240 activity on model disagreement, we assessed the correlation between distance to infrastructure
241 and model disagreement both for each plot and for a set of randomly sampled 10 x 10 km grid
242 cells.

243 **Results**

244 Model performance

245 The average performance of our models was 0.58 Spearman correlation (0.59 Spearman
246 correlation or 8.3 mean absolute error without GLM) and 8.1 mean absolute error. The best
247 model was GBM which had 0.61 Spearman correlation and the lowest mean absolute error
248 (7.9). For model fits to be considered for spatial projections and subsequent analyses, we
249 defined a Spearman correlation coefficient of 0.55 as minimum model performance. We
250 therefore removed GLM model from the ensemble predictions, due to too low performance.

251 Role of selected predictors

252 The predictive power of environmental variables shows that climate-related factors are better
253 predictors of mean community-level plant species richness than factors related to topography or
254 of human influence (Table 2). Our results confirm that community-level species richness in the
255 Arctic is strongly linked to warmth, but the actual dependence is unexpected: lower mean
256 ground temperature and fewer growing degree days are associated with higher species
257 richness (found primarily in the more continental Gydan peninsula) (Appendix Fig. 2). The trend
258 is different for low mean temperature of driest quarter (spring) where highest species richness is
259 associated with intermediate temperatures (Appendix Fig. 2). Moisture factors are also
260 important: the maximum and range of the climate moisture index as well as potential
261 evapotranspiration (min) significantly contribute to model quality (Appendix Fig. 2). Cloud area
262 fraction and mean wind speed show moderate predictive power (5 and 7% respectively). High
263 species richness is associated with relatively low wind speed and cloud fraction (Appendix Fig.
264 2). Topographic relief factors are generally less important for community-level species richness
265 than climate variables. Plant species richness has a positive correlation with slope and standard
266 deviation of altitude (Appendix Fig. 2). They are the only two topographic relief predictors which
267 have predictive power higher than 5%. Altitude, aspect, topographic wetness index and
268 roughness (topographic position index), on the other hand, have very low predictive power. Plot
269 size was omitted as a predictor during GAM and GLM stepwise variable reduction, so we
270 consider the plot size effect as minor as long as the plot size is not enlarged further. Multivariate
271 GBM and RF also show the same model performance with and without the use of plot size.

272

273 Paleoclimatic predictors

274 Paleoclimatic predictors show high predictive power, partly even higher than any contemporary
275 temperature predictor used, yet they are strongly correlated with modern climate predictors. The

276 strongest paleoclimate predictor found is temperature from 12.1 thousand years ago, which
277 alone explains 24.6% of the deviance (4.5% higher than that of the actual mean annual air
278 temperature). The next four strongest paleo-predictors are also temperatures from the
279 Pleistocene-Holocene boundary period (11.2-12.7 thousand years ago), which all demonstrate
280 high predictive power (24.5-25.5% explained deviance). At the same time, all the strongest
281 paleoclimatic predictors (temperature, precipitation, distance to land ice) exhibit high correlation
282 with current mean ground temperature (0.95, 0.83 and 0.72 respectively for a 12.1-thousand-
283 year-old time point) and often among each other. The data show no evidence of either land ice
284 or sea water at the plot locations throughout the entire time period, though the altitude data
285 seems to have low accuracy. The closest points to the continental ice are found to be Bely
286 Island (180 km) and Nakhodka bay (Southern Yamal) (200 km).

287

288 Spatial patterns of community-level plant species richness

289 Our model results show a highly heterogeneous distribution of community-level plant species
290 richness across the Western Siberian tundra (Fig. 2). Mean species richness of the model
291 ensemble map varies from 20 species on Eastern Yamal, Bovanenkovo railroad area (Fig. 2, 4),
292 to more than 40 in the Gydan national park area. The Yamal peninsula shows generally lower
293 species richness than Gydan. Furthermore, longitudinal differences between Yamal and Gydan
294 are generally higher than latitudinal differences within both peninsulas. Protected areas (except
295 Gydan National park) generally cover areas with low species richness. At the same time, the
296 main part of the species-rich area in Northern Gydan remains unprotected as well as smaller
297 species-rich areas in Northern and Eastern Yamal.

298

299 Community-level plant species richness across the Western Siberian tundra does not
300 decline with latitude

301 It is widely recognized that landscape-level or regional plant species richness in the Arctic
302 tundra is strongly dependent on summer warmth and hence declines with latitude (Hypothesis
303 3). At the community level, we found an opposing trend: median species richness of lichens,
304 mosses, and vascular plants increases with latitude (reduced warmth) (Fig. 2). As single
305 predictor, latitude is a relatively strong predictor of community-level plant species richness
306 across the area with 15% of deviance explained (Appendix Table S1). Given the high correlation
307 of latitude with other, more direct predictors, it was not used in the final model but we clearly see
308 a temperature-richness effect that is opposed to the expected decline on richness with latitude
309 and associated decrease in temperatures.

310

311 Model disagreement and its spatial patterns

312 The ensemble of models shows low model disagreement (less than 6 species) in most parts of
313 Gydan, Taz peninsula and some areas of Northern, Southern and coastal Eastern Yamal (Fig.
314 3). We identified high model uncertainty (7-14 species) in the Western and Central Yamal,
315 around Novy port and the South Tambey gas field at the eastern coast of Yamal, and on both
316 the Taz bay and on Bely island. All the areas with high model uncertainty apart from Bely Island
317 are exposed to high anthropogenic impacts, so we additionally assessed the correlation
318 between distance to infrastructure and model disagreement. Low positive correlation is present
319 for both plot locations (0.39) and among randomly selected sites (0.3).

320

321 Anthropogenic impact as a predictor

322 To estimate the influence of anthropogenic impact on species richness we tested distance to
323 infrastructure as a predictor, which has significant predictive power (12% explained deviance).
324 The GAM response curve shows that the dependence of species richness from distance to
325 infrastructure is non-linear whereby the closest and furthest located sites are associated with

326 highest species richness (Appendix Fig. 2). By contrast, the lowest species richness is
327 associated with sites at intermediate distances (30 to 50 km).

328 The role of anthropogenic factors in shaping plant species richness is underlined by model
329 projections. We tested two mapping options: (1) using the actual distance to infrastructure raster
330 (Fig. 4) and (2) using a hypothetical zero human impact raster (distance to infrastructure was
331 set to maximum value) (Fig. 5). We also calculated maximum disagreement between
332 projections of these 2 options and their uncertainties (Appendix Fig. 3). In contrast to the
333 'environmental only' and the 'actual distance to infrastructure' projections, the map of 'zero
334 human impact' shows relatively high species richness across vast areas of Yamal (especially in
335 the South) and low species richness in South-Eastern Gydan. The 'actual distance to
336 infrastructure' projection shows circular patterns of species richness around some infrastructure
337 objects clearly present in Western and Central Yamal, but also in some areas in Taz and Gydan
338 (Fig. 4). Model disagreement within the 'zero human impact' projection is significantly higher (up
339 to more than 30 species in some areas of Southern Gydan and Central Yamal) than the 'actual
340 distance to infrastructure' and the 'environmental-only' projections which have similar numbers
341 (up to 12 species) and spatial patterns (Figs 3-5).

342 An additional test on model disagreements between 'actual distance to infrastructure', 'zero
343 human impact' and 'environmental-only' projections shows that highest model uncertainty is
344 associated with intermediate and sometimes neighboring distances (Appendix Fig. 3).

345 **Discussion**

346 Our models show a highly heterogeneous distribution of community-level plant species richness
347 across the Western Siberian tundra. In the study, we tested four hypotheses. As we expected in
348 H.1, climate factors such as ground temperature and precipitation play a key role in shaping
349 community species richness while topographic relief plays a secondary role (Table 2). Contrary
350 to the pattern common in the Arctic on the regional level, we do not find a decrease in

351 community-level species richness from South to North, but rather a consistent increase (H.2,
352 Fig. 2). While being less important than environmental factors, anthropogenic impacts
353 (measured as spatial distance to infrastructures) contribute to the spatial heterogeneity of
354 species richness, whereby their impact is strongest in the southwestern part of the area and
355 some parts of southern Gydan (H.3, Fig. 4-5; Appendix Fig. 3). It is identified as one of the
356 factors that removes uncertainty in the results, increasing species richness close to
357 infrastructure and decreasing it at intermediate distances (Fig. 4-5, Appendix Fig. 3) compared
358 to large distances. Our results reveal the complex interplay of factors driving community species
359 richness in the Western Siberian tundra, which include both natural and anthropogenic forces
360 interacting with each other. Finally, in accordance with H.4, our results suggest that the most
361 species-rich areas remain largely unprotected (Fig. 2).

362
363 Our results suggest increasing mean community-level species richness from South-West to
364 North-East which does not fit well with the common view of a clear negative latitudinal richness
365 gradient in the Arctic (Daniëls et al. 2000; Shultz, 2005; Walker et. al, 2005; Daniëls et al.,
366 2013), but is in agreement with some earlier studies made on the site-level in Western Siberia
367 (Khitun, 1998; Rebristaya, 2013). Potential explanations relate to the history and geography of
368 the region. Northern Gydan, which contained refugia during the last ice age (Khitun, 1998), has
369 a higher richness than the Yamal peninsula. The latter was completely covered by water during
370 the middle Pleistocene and mostly during the late Pleistocene transgressions, while Gydan kept
371 the terrestrial connections with relatively rich Taymyr and Central Siberian floras (Khitun, 1998;
372 Rebristaya, 2013). The North-east of Gydan is also characterized by soils generally less acidic
373 than Yamal, permitting several arctic-alpine species to migrate from the east and settle there
374 (Khitun, 1998; CAVM, 2003). These idiosyncratic histories and connections may partly explain
375 the reversal of the South-North trend there (Khitun, 1998). However, we do not detect an
376 equally strong and consistent South-to-North increase in Yamal (Fig. 2, Fig. 4). But even here,

377 the projected community species richness is lowest in the southern part, which is at the same
378 time the most well-connected area of the peninsula, adjacent to the Polar Urals. Hence, the
379 complex factors are influencing this pattern, which were confirmed by our analysis.

380

381 The testing of historical climate predictors indicate that paleoclimate had a significant impact on
382 plant species richness distribution, with paleoclimate predictors such as temperature and
383 precipitation sometimes being more significant than the similar contemporary climate predictors
384 which indicates a legacy effect of past climate on the contemporary, community-level richness
385 patterns. According to the CHELSA-TraCE21k dataset our study area was not affected by
386 glaciation or sea level change over the past 21,000 years, which differs from previous research
387 on the region that indicated some sea transgressions during the Boreal age of Holocene (9,200-
388 8,200 years ago), although not as significant as those in the Pleistocene (Rebristaya, 2013). It is
389 challenging to separate the influence of current climate from the history of the area, as
390 demonstrated at the example of Gydan, where the high species richness is mostly attributed to
391 its historical development (Khitun, 1998).

392

393 The patchy but rather low predicted species richness in the southern and western parts of the
394 study area (especially in southern Yamal) might also be partly a result of anthropogenic
395 vegetation change through a combination of intense reindeer herding and gas extraction
396 (Golovatin et al., 2010; Ektova and Morozova, 2015; Forbes, 2013; Golovnev et al., 2016,
397 Veselkin et al., 2021). The expansion of oil and gas infrastructure drives changes in ecological
398 communities on a broad spatial scale, through associated species invasions and reducing
399 reindeer grazing ground (down to 50-90% within 3-10 km) at short distances and resulting
400 increase of reindeer density at intermediate distances (Kryazhimskii et al., 2011; Nellemann et
401 al. 2001). Gas drilling is currently expanding in Northern Gydan which could further endanger
402 the most species-rich ecosystems only partially protected by Gydan National Park. Our model

403 results indicate that more targeted research is needed to investigate the direct and indirect
404 impact of human activities such as industrial expansion and related herding density change, and
405 how they affect plant species richness. Social studies suggest that in Yamal increased pressure
406 on pastures could be driven by land deprivation, pushing the herders to graze reindeers on
407 smaller fields (Forbes, 2013) which in turn could lead to plant diversity loss.

408
409 Plant species richness across the Western Siberian tundra is shaped by a combination of
410 environmental and anthropogenic factors, whereby the influence of climate factors is the
411 strongest. The capacity of nature reserves to protect plant species is limited because of their
412 insufficient spatial coverage, low connectivity, sole focus on animal protection in some cases,
413 and often weak protection status (Kalyakin et al. 2000; Barry et al., 2017). Therefore, plant
414 diversity protection requires a complex social-ecological approach that is up to be developed.
415 Reducing industrial activity and active participation of Nenets people should be part of the
416 approach.

417

418 **Supporting information**

419 APPENDIX FIGURE 1: Distance to infrastructure (km) map.

420 APPENDIX FIGURE 2: GAM response curves.

421 APPENDIX FIGURE 3. Additional distance to infrastructure test results.

422 APPENDIX Table S1: Full list of tested predictors

423 APPENDIX S2: ODMAP protocol

424 **References**

425 Arctic Council, Conservation of Arctic Flora and Fauna Working Group (2010). CAFF Map
426 No.58 - Protected Areas in the Arctic classed after their IUCN category.

427 Arefev, S.P., Bogdanov, V.D., Golovatin, M.G., Gorbunov, P.Yu., Grigoreva, O.V., Dyachenko,
428 A.P., Ermakov, A.M., Ishenko, V.G., Zinovev, E.V., Zoteeva, E.A. and Knyazev, M.S., 2010.
429 Red book of Yamalo-Nenets Autonomous District: animals, plants, fungi. [Arefev, S.P.,
430 Bogdanov, V.D., Golovatin, M.G., Gorbunov, P.Yu., Grigoreva, O.V., Dyachenko, A.P.,
431 Ermakov, A.M., Ishenko, V.G., Zinovev, E.V., Zoteeva, E.A. and Knyazev, M.S., 2010. Krasnaya
432 kniga Yamalo-Neneckogo avtonomnogo okruga: zhivotnye, rasteniya, griby.]

433 Barry, T., Hólmgímur, H., & Guðmundsdóttir S. (2017). Arctic protected areas in 2017: status
434 and trends. *Biodiversity*, 18(4), 186–195. <https://doi.org/10.1080/14888386.2017.1390496>

435 Bivand, R., Keitt, T., & Rowlingson, B. (2021). rgdal: Bindings for the 'Geospatial' Data
436 Abstraction Library <https://CRAN>.

437 Broennimann, O., Di Cola, V., Petitpierre, B., Breiner, F., Scherrer, D., Manuela, D., Randin, C.,
438 Engler, R., Hordijk, W., Mod, H., & Pottier, J. (2014). Package 'ecospat'.

439 Brun, P., Zimmermann, N.E., Hari, C., Pellissier, L., & Karger, D.N. (2022). Global climate-
440 related predictors at kilometre resolution for the past and future, *Earth Syst. Sci. Data Discuss.*
441 [preprint], <https://doi.org/10.5194/essd-2022-212>, in review.

442 CAVM team (2003). Circumpolar Arctic vegetation map." Conservation of Arctic Flora and
443 Fauna (CAFF) Map No 1.

444 Chernyadyeva, I.V. (2001). Moss flora of Yamal Peninsula (West Siberian Arctic). *Arctoa*, 10,
445 121. [10.15298/arctoa.10.13](https://doi.org/10.15298/arctoa.10.13)

446 Conservation of Arctic Flora and Fauna (CAFF). (1997) CPAN Progress Report 1997. 39.

447 Daniëls, F.J.A., Bültmann, H., Lünterbusch, C., & Wilhelm, M. (2000). Vegetation zones and
448 biodiversity of the North American Arctic. *Ber. Reinh. Tuxen Ges.*, 12, 131–151.

449 Daniëls, F.J.A., Elvebakk, A., Talbot, S.S., & Walker, D.A. (2005). Classification and mapping of
450 arctic vegetation. *Phytocoenologia*, 35, 715–1079. [10.1127/0340-269X/2005/0035-0715](https://doi.org/10.1127/0340-269X/2005/0035-0715)

451 Daniëls, F.J.A., Gillespie, L.J., Poulin, M., Afonina, O.M., Alsos, I.G., Aronsson, M., Bültmann,
452 H., Ickert-Bond, S.M., Konstantinova, N., Lovejoy, C., & Väre, H. (2013). Chapter 9. Plants.,
453 *Arctic Biodiversity Assessment. Status and Trends in Arctic Biodiversity*, (pp. 258–301).
454 Conservation of Arctic Flora and Fauna (CAFF).

455 Egelkraut, D., Barthelemy, H., & Olofsson, J. (n.d.). Reindeer trampling promotes vegetation
456 changes in tundra heathlands: Results from a simulation experiment. *Journal of Vegetation*
457 *Science*, 31(3), 476–486.

458 Ektova, S. N., & Morozova, L. M. (2015). Rate of recovery of lichen-dominated tundra
459 vegetation after overgrazing at the Yamal Peninsula. *Czech Polar Reports*, 5(1), 27–32.

460 Elven, R. (2011). Annotated checklist of the Panarctic Flora (PAF).

461 Forbes, B.C. (1995) Tundra disturbance studies. III. Short-term effects of aeolian sand and dust,
462 Yamal Region, northwest Siberia, Russia. *Environmental Conservation* 22: 335-344.
463 <https://doi.org/10.1017/S0376892900034901>.

464 Forbes, B.C. (1997) Tundra disturbance studies. IV. Species establishment on anthropogenic
465 primary surfaces, Yamal Peninsula, northwest Siberia, Russia. *Polar Geography* 21: 79-100.
466 <https://doi.org/10.1080/10889379709377619>.

467 Forbes, B.C. and O.I. Sumina. (1999). Comparative ordination of low arctic vegetation
468 recovering from disturbance: Reconciling two contrasting approaches for field data collection.
469 *Arctic, Antarctic and Alpine Research*, 31, 389–399.
470 <https://doi.org/10.1080/15230430.1999.12003323>

471 Forbes, B.C. (2013). Cultural resilience of social-ecological systems in the Nenets and Yamal-
472 Nenets Autonomous Okrugs, Russia: a focus on reindeer nomads of the tundra. *Ecology and*
473 *society*, 18(4). <http://dx.doi.org/10.5751/ES-05791-180436>

474 Forbes, B.C., Stammer, F., Kumpula, T., Meschtyb, N., Pajunen, A., & Kaarlejärvi, E. (2009).
475 High resilience in the Yamal-Nenets social–ecological system, West Siberian Arctic, Russia.
476 *Proceedings of the National Academy of Sciences*, 106(52), 22041–22048.
477 <https://doi.org/10.1073/pnas.0908286106>

478 Golovatin, M. G., Morozova, L. M., Ektova, S. N., & Paskhalny, S. P. (2010). The change of
479 tundra biota at Yamal peninsula (the North of the Western Siberia, Russia) in connection with
480 anthropogenic and climatic shifts. *Tundras: Vegetation, wildlife and climate trends*. New York:
481 Nova Publishers, 1–46.

482 Golovatin, M., Morozova, L., & Ektova, S. (2012). Effect of reindeer overgrazing on vegetation
483 and animals of tundra ecosystems of the Yamal peninsula. *Czech Polar Reports*, 2(2), 80–91.
484 <https://doi.org/10.5817/CPR2012-2-8>

485 Golovnev, A.V., Garin, N.P., & Kukanov, D.A. (2016). Olenevody Yamala (materialy k Atlasu
486 kochevyh tekhnologij) [Reindeer herders of Yamal (materials for the Atlas of nomadic
487 technologies)]. UrO RAS Publ.

488 Greenwell, B., Boehmke, B., Cunningham, J., & GBM Developers (2020). gbm: Generalized
489 Boosted Regression Models. R package version 2.1.8.

490 Guisan, A., & Rahbek, C. (2011). SESAM – a new framework integrating macroecological and
491 species distribution models for predicting spatio-temporal patterns of species assemblages.
492 *Journal of Biogeography*, 38(8), 1433-1444. <https://doi.org/10.1111/j.1365-2699.2011.02550.x>

493 Guisan, A., Thuiller, W., & Zimmermann, N.E. (2017). *Habitat suitability and distribution models:*
494 *with applications in R.*, Cambridge University Press. <https://doi.org/10.1017/9781139028271>

495 Hastie, T. (2020). gam: Generalized Additive Models. R package version 1.20.

496 Hijmans, R.J., Van Etten, J., Cheng, J., Mattiuzzi, M., Sumner, M., Greenberg, J.A., Lamigueiro,
497 O.P., Bevan, A., Racine, E.B., Shortridge, A., & Hijmans, M.R.J. (2015). Package 'raster'.

498 Iturrate-Garcia, M., O'Brien, M.J., Khitun, O., Abiven, S., Niklaus, P.A., & Schaeppman-Strub, G.
499 (2016). Interactive effects between plant functional types and soil factors on tundra species
500 diversity and community composition. *Ecology and evolution*, 6(22), 8126–8137.
501 <https://doi.org/10.1002/ece3.2548>

502 Kalyakin, V.N., Romanenko, F.A., Molochaev, A.V., Rogacheva, E.V., & Syroechkovskii, E.E.
503 (2000). Gydanskiy zapovednik [Gydan natural reserve], in Zapovedniki Sibiri [Natural reserves
504 of Siberia], 2, pp. 47–55.

505 Karger, D.N., Conrad, O., Böhner, J., Kawohl, T., Kreft, H., Soria-Auza, R.W., Zimmermann,
506 N.E., Linder, H.P., & Kessler, M. (2016). CHELSA climatologies at high resolution for the earth's
507 land surface areas (Version 1.0).

508 Karger, D.N., Conrad, O., Böhner, J., Kawohl, T., Kreft, H., Soria-Auza, R.W., Zimmermann,
509 N.E., Linder, H.P., & Kessler, M. (2017). Climatologies at high resolution for the earth's land
510 surface areas. *Scientific data*, 4(1), 1–20. <https://doi.org/10.1038/sdata.2017.122>

511 Karger, D. N., Nobis, M. P., Normand, S., Graham, C. H., & Zimmermann, N. E. (2021):
512 CHELSA-TraCE21k v1. 0. Downscaled transient temperature and precipitation data since the
513 last glacial maximum. *Climate of the Past Discussions*, 1-27.

514 Khitun, O.V. (1998). Sravnitelnyy analiz lokalnykh i partsialnykh flor v dvukh podzonakh
515 Zapadnosibirskoy Arktiki (p-ova Gydanskiy i Tazovskiy) [Comparative analysis of local and
516 partial floras in two subzones of the West Siberian Arctic (the Gydan and Taz Peninsulas)].
517 *Study of biological diversity by the methods of comparative floristics: Materials of the IV*
518 *workshop on comparative floristics.*, 173–201.

519 Khitun, O.V. (2002). Vnutrilandshaftnaya struktura flory okrestnostey ustia reki Tinikiyakha
520 (severnnyye gipoarkticheskiye tundry Gydanskogo poluostrova) [Intralandscape structure of flora
521 of the surroundings of the Tinikiyakha River mouth (northern hypoarctic tundra in the Gydanskii
522 Peninsula)]. *Botanicheskii zhurnal*, 87(8), 1–24.

523 Khitun, O.V. (2003). Analiz vnutrilandshaftnoy struktury flory srednego techeniya reki
524 Khalmeryakha (Gydanskiy p-ov) [Analysis of the intralandscape structure of flora of the
525 Khalmeryakha middle reaches (Gydansky Peninsula)]. *Botanicheskii zhurnal*, 88(10), 21–39.

526 Khitun, O.V. (2016). Intralandscape differentiation of the local flora in the central part of the
527 Gydansky Peninsula (West Siberian Arctic). *Czech Polar Reports*, 6(2), 191–209.
528 <https://doi.org/10.5817/CPR2016-2-18>

529 Khitun, O.V., & Rebristaya, O.V. (1998). Rastitelnost' i ekotopologicheskaya struktura flory
530 okrestnostey mysy Khonorasale (arkticheskiye tundry Gydanskogo poluostrova). [Vegetation
531 and ecotopological structure of Khorosale cape surroundings flora (arctic tundra of Gydan
532 peninsula)]. *Botanicheskii Zhurnal*, 83(12), 21–37.

533 Khitun, O.V., Koroleva, T.M., Chinenko, S.V., Petrovsky, V.V., Pospelova, E.B., Pospelov, I.N.,
534 & Zverev, A. (2016). Applications of local floras for floristic subdivision and monitoring vascular
535 plant diversity in the Russian Arctic. *Arctic Science*, 2(3), 103–126. [https://doi.org/10.1139/as-](https://doi.org/10.1139/as-2015-0010)
536 [2015-0010](https://doi.org/10.1139/as-2015-0010)

537 Koroleva, T.M., Zverev, A.A., Katenin, A.E., Petrovskii, V.V., Pospelova, E.B., Rebristaya, O.V.,
538 Khitun, O.V., Khodachek, E.A. & Chinenko, S.V. (2011). *Botanicheskii zhurnal*, 96(2)
539 (Dolgotnaya geograficheskaya struktura lokalnykh i regionalnykh flor Aziatskoy Arktiki. 2.
540 [Longitudinal geographic structure of local and regional floras of the Asian Arctic. 2.]), 145–169.

541 Kozlova, A.E. (2013). Antropogennoe preobrazovaniye relief v usloviakh khozyaistvennogo
542 osvoeniya territorii poluostrova Yamal. [Anthropogenic relief change during the economic
543 development of Yamal]. *Izvestiya Rossiyskoy akademii nauk*, 4, 87–94.

544 Kryazhimskii, F. V., Maklakov, K. V., Morozova, L. M., & Ektova, S. N. (2011). System analysis
545 of biogeocenoses of the Yamal Peninsula: Simulation of the impact of large-herd reindeer
546 breeding on vegetation. *Russian Journal of Ecology*, 42(5), 351–361. Kumpula, T., Forbes,
547 B.C., Stammer, F., & Meschtyb, N. (2012). Dynamics of a coupled system: multi-resolution
548 remote sensing in assessing social-ecological responses during 25 years of gas field
549 development in Arctic Russia. *Remote Sensing*, 4(4), 1046–1068.
550 <https://doi.org/10.3390/rs4041046>

551 Kumpula, T., Pajunen, A., Kaarlejärvi, E., Forbes, B.C., & Stammer, F. (2011). Land use and
552 land cover change in Arctic Russia: Ecological and social implications of industrial development.
553 *Global Environmental Change*, 21(2), 550–562. <https://doi.org/10.1016/j.gloenvcha.2010.12.010>

554 Liaw, A. & Wiener, M. (2002). Classification and Regression by Random Forest. *R News*, 2, 18-
555 22.

556 Magomedova, M.A., Morozova, L.M., Ektova, S.N., Rebristaya, O.V., Chernyadyeva, I.V.,
557 Potemkin, A.D., & Knyazev, M.S. (2006). *Poluostrov Yamal: rastitelniy pokrov [The Yamal*
558 *Peninsula: vegetation cover]*, City-press.

559 Marthews, T. R., Dadson, S. J., Lehner, B., Abele, S., & Gedney, N. (2015). High-resolution
560 global topographic index values. NERC Environmental Information Data
561 Centre. <https://doi.org/10.5285/6b0c4358-2bf3-4924-aa8f-793d468b92be>

562 Matveeva, N.A. (1998). *Zonalnost' v rastitelnom pokrove Arktiki. [Zonation in the plant cover in*
563 *the Arctic]*, BIN RAN.

564 Morin, P., Porter, C., Cloutier, M., Howat, I., Noh, M.J., Willis, M., Bates, B., Williamson, C. &
565 Peterman, K. (2016). ArcticDEM: a publically available, high resolution elevation model of the
566 Arctic. *Egu general assembly conference abstracts*.

567 Nellemann, C. et al. (2001) GLOBIO Global methodology for mapping human impacts on the
568 biosphere: the Arctic 2050 scenario and global application. UNEP/DEWA Technical Report 3,
569 47 pp.

570 Obu, J., Westermann, S., Bartsch, A., Berdnikov, N., Christiansen, H.H., Dashtseren, A.,
571 Delaloye, R., Elberling, B., Etzelmüller, B., Kholodov, A., & Khomutov, A. (2019). Northern
572 Hemisphere permafrost map based on TTOP modelling for 2000–2016 at 1 km² scale. *Earth-*
573 *Science Reviews*, 193, 299-316. <https://doi.org/10.1016/j.earscirev.2019.04.023>

574 Porter, C., Morin, P., Howat, I., Noh, M.J., Bates, B., Peterman, K., Keesey, S., Schlenk, M.,
575 Gardiner, J., Tomko, K., & Willis, M. (2018). ArcticDEM, V1, Harvard Dataverse.
576 <https://doi.org/10.7910/DVN/OHHUKH>

577 Povoroznyuk, O., Vincent, W.F., Schweitzer, P., Laptander, R., Bennett, M., Calmels, F.,
578 Sergeev, D., Arp, C., Forbes, B.C., Roy-Léveillé, P. & Walker, D.A. (2022). Arctic roads and
579 railways: Social and environmental consequences of transport infrastructure in the circumpolar
580 North. *Arctic Science*. <https://doi.org/10.1139/AS-2021-0033>

581 QGIS Development Team (2022). QGIS Geographic Information System. Open Source
582 Geospatial Foundation Project. Version 3.12. Retrieved June 30, 2022, from
583 <http://qgis.osgeo.org>.

584 Reynolds, M.K., Breen, A.L., Walker, D.A., Elven, R., Belland, R., Konstantinova, N.,
585 Kristinsson, H., & Hennekens, S. (2013). The Pan-Arctic Species List (PASL). *Arctic Vegetation*
586 *Archive (AVA) Workshop*.

587 Rebristaya, O.V. (1995). Vascular plants of the Bely Island (Kara Sea). *Botanicheskii zhurnal*,
588 80(7), 16–36.

589 Rebristaya, O.V. (2013). *Flora poluostrova Yamal: sovremennoye sostoyaniye i istoriya*
590 *formirovaniya. [Flora of the Yamal peninsula: modern state and history of the formation]*, Izd-vo
591 SPbGETU «LETI».

592 Rebristaya, O.V., & Khitun, O.V. (1998). Botaniko-geograficheskiye osobennosti flory
593 Tsentralnogo Yamala [Botanical-geographic peculiarities of the flora of Central Yamal].
594 *Botanicheskii zhurnal*, 83(7), 37–52.

595 Rebristaya, O.V., & Khitun, O.V. (1994). Flora sosudistykh rasteniy nizovyev reki Chugoriakha
596 (yugo-zapadnaya chast Gydanskogo poluostrova. Zapadnosibirskaya Arktika). [Vascular plants
597 flora of the lower reaches of the Chugoryakha River (south-western part of the Gydansky
598 Peninsula, Western Siberian Arctic)]. *Botanicheskii Zhurnal*, 79(8), 68–77.

599 Rebristaya, O.V., Tvorogov, V.A., & Khitun, O.V. (1989). Flora Tazovskogo poluostrova (sever
600 Zapadnoy Sibiri) [Flora of the Tazovsky Peninsula (north of the Western Siberia)]. *Botanicheskii*
601 *zhurnal*, 74(1), 22–35.

602 Schultz, J. (2005). *The ecozones of the world.*, Springer. <https://doi.org/10.1007/3-540-28527-X>

603 Sekretareva, N.A. (1999). *The vascular plants of the Russian Arctic and adjacent territories.*,
604 Pensoft.

605 Skipin, L.N., Galyamov, A.A., Gaevaya, E.V., & Zakharova, E.V. (2014). Ekologicheskaya
606 otsenka sostoyaniya pochvennogo pokrova oleniikh pastbish poluostrova Yamal [The ecological
607 assessment of reindeer pastures soils of the Yamal peninsula]. *Agroprodovolstvennaya politika*
608 *Rossii*, 4, 29–32.

609 Stewart, L., Alsos, I.G., Bay, C., Breen, A.L., Brochmann, C., Boulanger-Lapointe, N.,
610 Broennimann, O., Bültmann, H., Bøcher, P.K., Damgaard, C., & Daniëls, F.J. (2016). The
611 regional species richness and genetic diversity of Arctic vegetation reflect both past glaciations
612 and current climate. *Global Ecology and Biogeography*, 25(4), 430–442.
613 <https://doi.org/10.1111/geb.12424>

614 Veselkin, D., Morozova, L., & Gorbunova, A. (2021). Decrease of NDVI values in the southern
615 tundra of Yamal in 2001–2018 correlates with the size of domesticated reindeer population.
616 *Mod. Probl. Remote Sens. Earth Space*, 18, 143-155. [https://doi.org/10.21046/2070-7401-2021-](https://doi.org/10.21046/2070-7401-2021-18-2-143-155)
617 [18-2-143-155](https://doi.org/10.21046/2070-7401-2021-18-2-143-155)

618 Voronova, O.G., & Diachenko, A.P. (2018). Bryophyte flora of hydrocarbon deposit sites in the
619 Yamalo-Nenets Autonomous Okrug. *Vestnik Tomskogo gosudarstvennogo universiteta*.
620 *Biologiya*, 42. <https://doi.org/10.17223/19988591/42/6>

621 Walker, D.A., Breen, A.L., Reynolds, M.K., & Walker, M.D. (2013). Arctic Vegetation Archive
622 (AVA) Workshop.

623 Walker, D.A., Daniëls, F.J., Matveyeva, N.V., Šibík, J., Walker, M.D., Breen, A.L.,
624 Druckenmiller, L.A., Reynolds, M.K., Bültmann, H., Hennekens, S., & Buchhorn, M. (2018).

625 Circumpolar arctic vegetation classification. *Phytocoenologia*, 48(2), 181–201.
626 <https://doi.org/10.1127/phyto/2017/0192>

627 Walker, D.A., Daniëls, F.J.A., Alsos, I., Bhatt, U.S., Breen, A.L., Buchhorn, M., Bültmann, H.,
628 Druckenmiller, L.A., Edwards, M.E., Ehrich, D., & Epstein, H.E. (2016). Circumpolar Arctic
629 vegetation: a hierarchic review and roadmap toward an internationally consistent approach to
630 survey, archive and classify tundra plot data. *Environmental Research Letters*, 11(5), 055005.
631 <https://doi.org/10.1088/1748-9326/11/5/055005>

632 Walker, D.A., Epstein, H.E., Reynolds, M.K., Kuss, P., Kopecky, M.A., Frost, G.V., Daniëls,
633 F.J.A., Leibman, M.O., Moskalenko, N.G., Matyshak, G.V., & Khitun, O.V. (2012). Environment,
634 vegetation and greenness (NDVI) along the North America and Eurasia Arctic transects.
635 *Environmental Research Letters*, 7(1), 015504. <https://doi.org/10.1088/1748-9326/7/1/015504>

636 Walker, D.A., Epstein, H.E., Šibík, J., Bhatt, U., Romanovsky, V.E., Breen, A.L., Chasníková, S.,
637 Daanen, R., Druckenmiller, L.A., Ermokhina, K., & Forbes, B.C. (2019). Vegetation on mesic
638 loamy and sandy soils along a 1700-km maritime Eurasia Arctic Transect. *Applied vegetation
639 science*, 22(1), 150–167. <https://doi.org/10.1111/avsc.12401>

640 Walker, D.A., Reynolds, M.K., Daniëls, F.J., Einarsson, E., Elvebakk, A., Gould, W.A., Katenin,
641 A.E., Kholod, S.S., Markon, C.J., Melnikov, E.S., & Moskalenko, N.G. (2005). The circumpolar
642 Arctic vegetation map. *Journal of Vegetation Science*, 16(3), 267–282.
643 <https://doi.org/10.1111/j.1654-1103.2005.tb02365.x>

644 Walker, M.D., Daniëls, F.J.A., & van der Maarel, E. (1994). Circumpolar arctic vegetation –
645 Introduction and perspective. *Journal of Vegetation Science*, 5, 758–764.
646 <https://doi.org/10.1111/j.1654-1103.1994.tb00395.x>

647 Yurtsev, B.A. (1994). Floristic division of the Arctic. *Journal of Vegetation Science*, 5(6), 765–
648 776. <https://doi.org/10.2307/3236191>

649 Zemlianskii, V. , Ermokhina, K., Schaepman-Strub, G., Matveyeva, N., Troeva, E., Lavrinenko,
650 I., Telyatnikov, M., Pospelov, I., Koroleva, N., Leonova, N., Khitun, O., Walker, D., Breen, A.,
651 Kadetov, N., Lavrinenko, O., Ivleva, T., Kholod, S., Petrzhik, N., Kurysheva, M., Gunin, Y.,
652 Lapina, A., Korolev, D., Kudr, E., & Plekhanova, E.. Russian Arctic Vegetation Archive – a new
653 database of plant community composition and environmental conditions. *Global Ecology and*
654 *Biogeography*, in review.

655 Zurell, D., Franklin, J., König, C., Bouchet, P.J., Serra-Diaz, J.M., Dormann, C.F., Elith, J.,
656 Fandos Guzman, G., Feng, X., Guillera-Arroita, G., Guisan A., Leitão, P.J., Lahoz-Monfort, J.J.,
657 Park, D.S., Peterson, A.T., Rapacciuolo, G., Schmatz, D.R., Schröder, B., Thuiller, W., Yates
658 K.L., Zimmermann, N.E., Merow, C. (2020). A standard protocol for describing species
659 distribution models. *Ecography* 43, 1261-1277. DOI: 10.1111/ecog.04960

660 Global Wind Atlas. Retrieved June 30, 2022, from <https://globalwindatlas.info/>

661 Ermokhina K., Zemlianskii V., Kurysheva M., & Korolev D. Russian Arctic Vegetation Archive
662 website. Retrieved June 30, 2022, from <https://avarus.space/>

663 Open Street map. Retrieved June 30, 2022, from <https://www.openstreetmap.org>

664 ORNL DAAC 2018. MODIS and VIIRS Land Products Global Subsetting and Visualization Tool.
665 ORNL DAAC, Oak Ridge, Tennessee, USA. Retrieved Semtember 23, 2021
666 <https://modis.gsfc.nasa.gov/>

667 (1992) UN Convention on Biological diversity, CBD.Assmann J. CHARTER WP4 Holocene Cryo
668 DB v2. Retrieved January 25, 2023, from https://github.com/jakobjassmann/cryo_db_v2

669 **Data availability statement:** Data available from the Dryad Digital Repository
670 (<https://datadryad.org/stash/share/bFWEuics4IXhXfj2xvo4or1sUYa-WriskoaRUuoVdeU>)
671 (Zemlianskii et al., 2022).

672 **Figures and tables**

673 **Table 1:** Model performance statistics from 5-fold cross-validation (GLM = generalized linear
674 model, GAM = generalized additive model, GBM = gradient boosting machine). Red color
675 shows GLM, which we omitted because of its comparably low performance (<0.55 Spearman
676 correlation). The numbers in brackets indicate the change in performance upon adding the
677 "distance to infrastructure" predictor.

Model	Spearman correlation	Mean Absolute Error	Root Mean Square Error
GLM	0.53	8.4 (8.3)	10.8 (10.7)
Random Forest	0.59	8.1	10.3
GAM	0.59	8.0	10.2
GBM	0.60 (0.61)	7.9	10.1 (10.0)

678

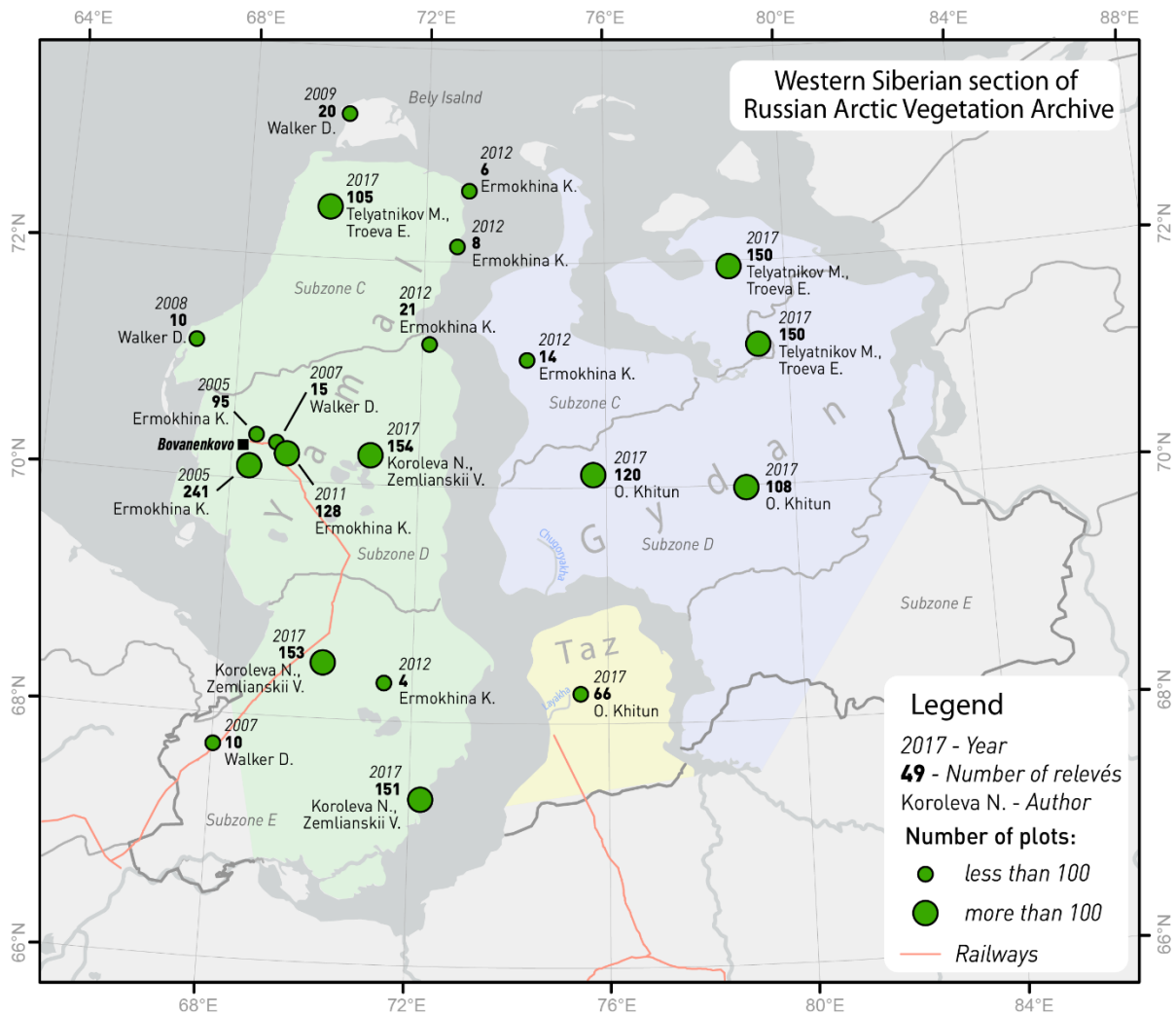
679 **Table 2:** Environmental variables used in the model. The full list of evaluated variables is
 680 presented in Appendix, Table 1.

N	Predictors	Predictive power (%)	Original spatial res. (m)	Source
1	Mean Ground Temperature (2000-2016)	19	1000	ESA Global permafrost project (Obu, et al., 2019)
2	Potential evapotranspiration (min)	17	30 arcsec (<1000)	CHELSA new (Brun et al., 2022)
3	Mean temperature of driest quarter	14	30 arcsec (<1000)	CHELSA Bioclim (Karger et al., 2016)
4	Climate moisture index (max)	13	30 arcsec (<1000)	CHELSA new (Brun et al., 2022)
5	Distance to infrastructure	11	1000	OSM based (https://www.openstreetmap.org/)
6	Growing degree days above 5°C	11	30 arcsec (<1000)	Extended Bioclim (Karger et al., 2017)
7	Climate moisture index (range)	11	30 arcsec (<1000)	CHELSA new (Brun et al., 2022)

8	(log transformed) slope	10	10	ArcticDEM based (Morin et al., 2016; Porter et al., 2018)
9	Cloud area fraction	7	30 arcsec (<1000)	CHELSA Bioclim (Karger et al., 2016)
10	Mean wind speed	5	100	Global Wind Atlas (https://globalwindatlas.info/)

681

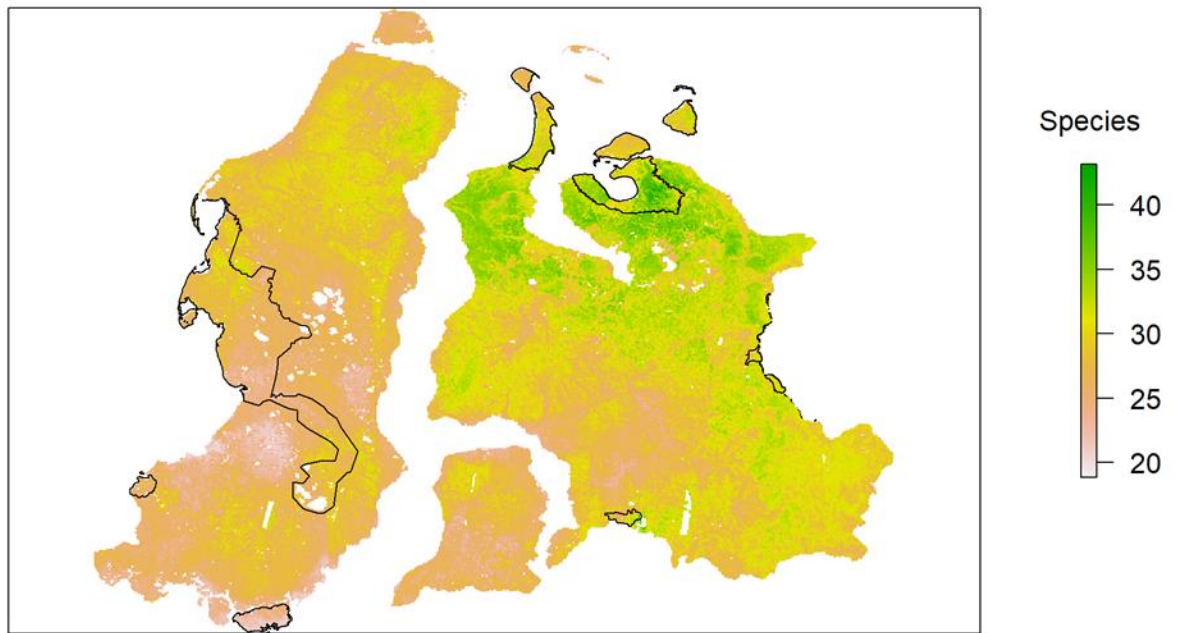
682



683

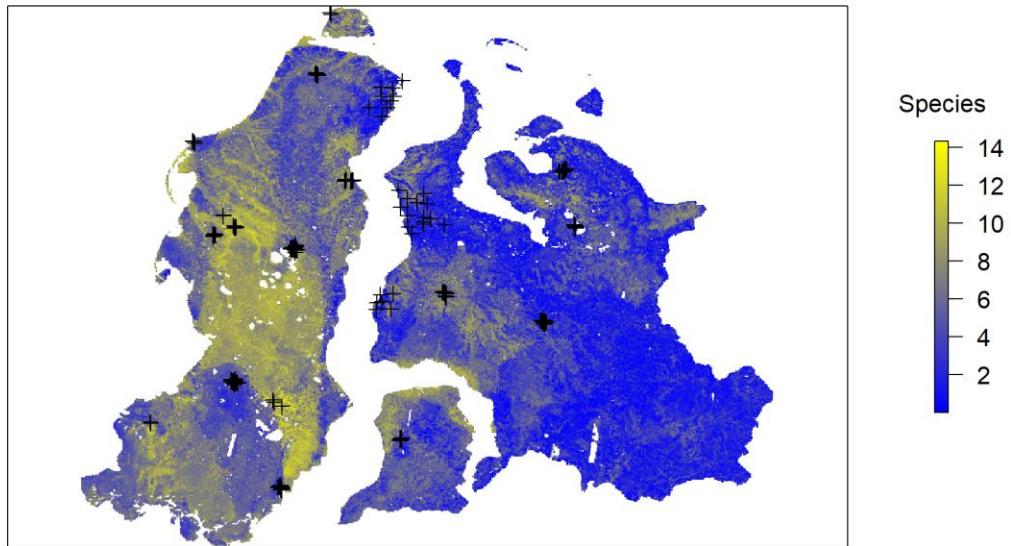
684 **Figure 1:** Western Siberian study area, including the location of the major study sites and respective number of geobotanical plots

685 per site (= number of relevés). The Yamal peninsula is shaded in green, Taz in yellow and Gydan in blue.



686

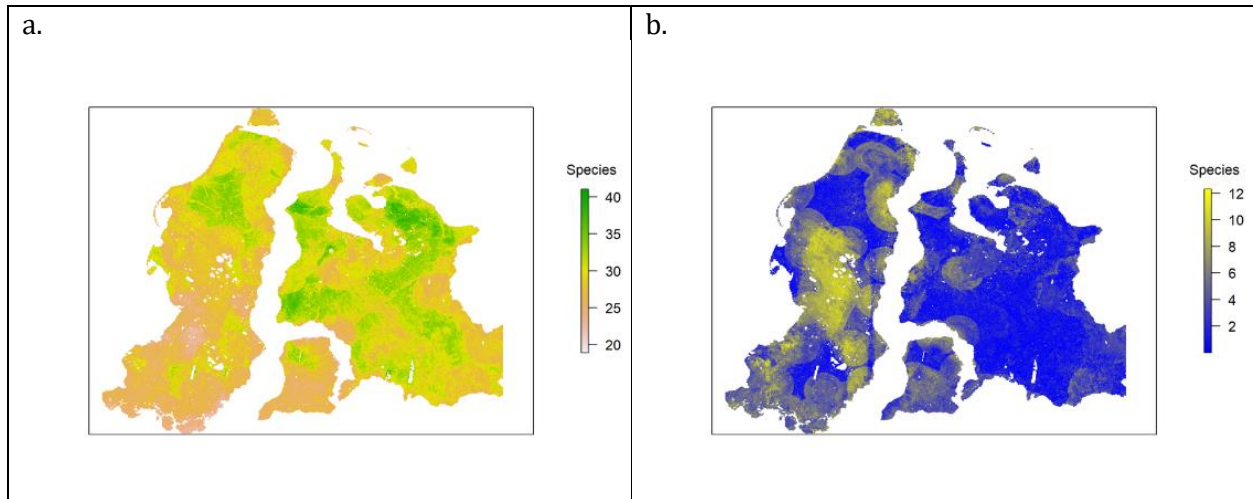
687 **Figure 2:** Mean plant species richness distribution in the Western Siberian tundra as predicted by a macroecological model
688 ensemble based on a general additive (GAM), gradient boosting machine (GBM) and random forest (RF) model. Black borders
689 show existing protected areas.



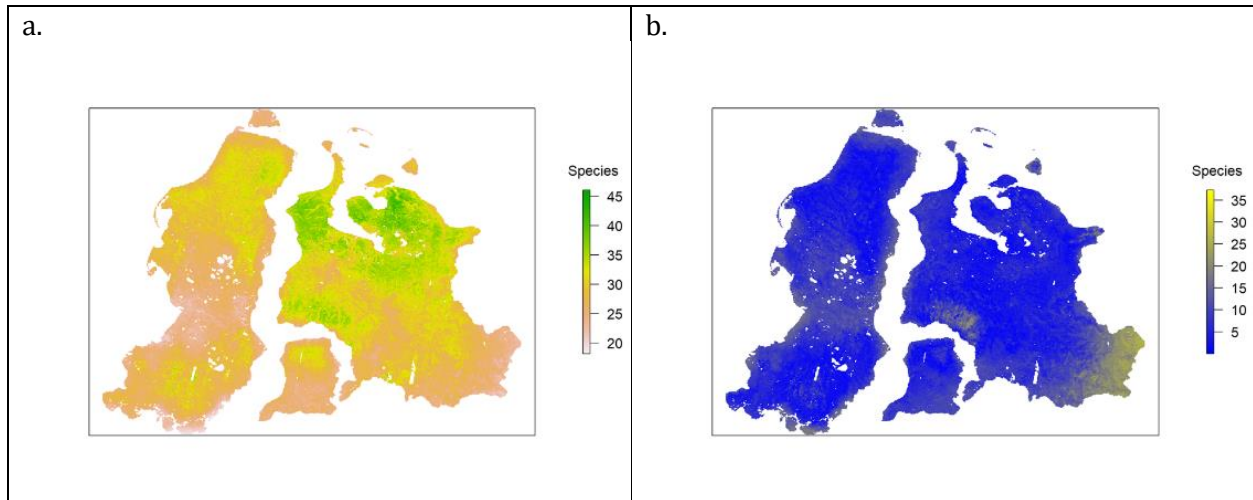
690

691 **Figure 3:** Model disagreement map indicating maximum difference in species number between GAM, GBM and Random forest
692 ('environmental only' projection). Black crosses are geobotanical plot locations.

693



694 **Figure 4.** "Actual distance to infrastructure" projection. **a.** Mean plant species richness distribution in the Western Siberian tundra as
 695 predicted by a macroecological model ensemble based on a general additive (GAM), gradient boosting machine (GBM) and random
 696 forest model, similar to Figure 2, but additionally including the predictor 'distance to infrastructure'. **b.** Model disagreement map
 697 indicating maximum difference in species number between general additive (GAM), gradient boosting machine (GBM) and random
 698 forest model) similar to Figure 3, but additionally including the predictor 'distance to infrastructure'.
 699



701 **Figure 5.** "Zero human impact" projection. **a.** Mean plant species richness distribution in the Western Siberian tundra as predicted
 702 by a macroecological model ensemble based on a general additive (GAM), gradient boosting machine (GBM) and random forest
 703 model, similar to Figure 2, but additionally including the predictor 'distance to infrastructure' set to the maximum value (115.285 km).
 704 **b.** Model disagreement map indicating maximum difference in species number between general additive (GAM), gradient boosting
 705 machine (GBM) and random forest model similar to Figure 3, but additionally including the predictor 'distance to infrastructure' set to
 706 the maximum value (115.285 km).